Karlsruhe Institute of Technology

Elektrotechnisches Institut (ETI)

Prof. Dr.-Ing. Martin Doppelbauer
Prof. Dr.-Ing. Marc Hiller

Kaiserstr.12. 76131 Karlsruhe

Elektrotechnisches Institut

Title:	Effects of Realistic Driving Profiles on the Degradation of Lithium-Ion Batteries
Authors:	Alexis Kalk, Marc Clemens Holocher, Sebastian Ohneseit, Christian Kupper, Marc Hiller
Institute:	Karlsruhe Institute of Technology (KIT) Elektrotechnisches Institut (ETI)
Type:	Conference Proceedings
Published at:	2023 IEEE International Transportation Electrification Conference (ITEC-India), 12-15 December 2023, Chennai, India Year: 2023 ISBN: 979-8-3503-3780-8
Hyperlinks:	DOI: 10.1109/ITEC-India59098.2023.10471482

Effects of Realistic Driving Profiles on the Degradation of Lithium-Ion Batteries

1st Alexis Kalk
Institute of Electrical Engineering (ETI)
Karlsruhe Institute of Technology (KIT)
Karlsruhe, Germany
alexis.kalk@kit.edu

2nd Marc Clemens Holocher
Institute of Electrical Engineering (ETI)
Karlsruhe Institute of Technology (KIT)
Karlsruhe, Germany

3rd Sebastian Ohneseit
Institute for Applied Materials (IAM-AWP)
Karlsruhe Institute of Technology (KIT)
Karlsruhe, Germany
sebastian.ohneseit@kit.edu

4th Christian Kupper
Institute of Electrical Engineering (ETI)
Karlsruhe Institute of Technology (KIT)
Karlsruhe, Germany
christian.kupper@kit.edu

5th Marc Hiller
Institute of Electrical Engineering (ETI)
Karlsruhe Institute of Technology (KIT)
Karlsruhe, Germany
marc.hiller@kit.edu

***Abstract*—This study explores the aging characteristics of lithium-ion batteries under conventional cycling tests and realistic driving profile tests. We employ regular capacity tests and electrochemical impedance spectroscopy for a comprehensive analysis of state of health. For this investigation, we used commercial, round $LiFePO_4$ cells in the 21700 format. The findings highlight more severe capacity loss under realistic driving profile tests compared to conventional cycling. This discrepancy hinting towards recuperation phases as a key factor in accelerated aging for lithium-ion batteries used in electric vehicles. This research underscores the importance of using realistic load scenarios for assessing battery life and may contribute to the development of more advanced battery management systems in electric vehicles.**

***Index Terms*—State of Health, Realistic Driving Profile, SOH, Aging, Electrochemical impedance spectroscopy, Lithium-Ion Battery**

I. Introduction

Lithium-ion battery (LIB) technology makes an important contribution to the electrification of the power train due to their high energy and power density, and long service time. However, despite these appealing characteristics, LIBs do experience a decline in their energy and power capacities over time and use. This phenomenon is referred to as battery degradation or aging. In the literature, two types of aging are identified, namely, calendar aging and cyclic aging. Calendar aging refers to time-related aging effects and cyclic aging describes the aging during usage. In general, capacity loss and increase of internal cell resistance are the two dominant indicators of battery aging. Understanding the degradation mechanisms of LIBs is crucial to enhance electric vehicle (EV) performance, reliability and cost-effectiveness.

The aging of LIBs is a highly complex process, influenced by numerous factors such as temperature, state of charge (SOC), charge-discharge rate (C-rate), depth of discharge (DOD), and number of cycles, among others. The term state of health (SOH) is used to describe the battery's degradation or aging state in percentage terms compared to the battery's initial properties. To discover the effects of the aging-relevant factors and the aging character of LIB, it is necessary to execute a comprehensive test matrix.

Unfortunately, the conventional aging tests are conducted in tightly controlled environments using synthetically defined test profiles, which inherently limit the ability to reproduce the variability of real-world driving scenarios. There are a limited number of studies in the existing literature that focus on this issue and its resultant effects. Panchal et al. [1] logged and utilized real driving data of an EV for the aging tests of a battery pack. The logged profile is 64 minutes long and covered a trip distance of 74 km. This profile is repeated over a three-month period on a test bench to observe the aging behaviour. However, this study did not include a comparison with standard aging tests or driving profile tests, nor did it provide a detailed analysis of the effects of real driving profiles on battery aging. Baure and Dubarry compared the effects of synthetic and real driving profiles on aging in their work [2]. They utilized cylindrical cells with NCA chemistry and employed incremental capacity analysis (ICA) technique to identify the effects on battery aging.

In this study, we concurrently executed conventional aging

tests and aging tests using generated realistic driving profiles on LFP ($LiFePO_4$) cylindrical cells with the aim to identify the effect of real-life conditions on battery aging. We utilized electrochemical impedance spectroscopy (EIS) as a tool to analyze these impacts on the aging of LIB. Following this introduction, we introduce first the applied methods for analysing battery degradation. Then, experimental setup and cell test profiles is described. In the final section, the results and the conclusions are presented.

II. Methods

A. Capacity Test

Capacity loss is one of the most common used indicators for degradation of the battery. Hence, we implemented capacity tests at fixed intervals to monitor changes in the battery's SOH. All the capacity tests are conducted at a controlled ambient temperature of $25\,^{\circ}\mathrm{C}$ in an incubator. The cells are charged utilizing constant current constant voltage (CC-CV) protocol with a constant current rate of $990\,\mathrm{mA}$ and discharged with a constant discharge current of $990\,\mathrm{mA}$. The actual available capacity Q_{act} is calculated with Coulomb Counting method. A measurement was taken at the beginning of the test campaign to establish the cell's reference available capacity Q_{ref}. The SOH is calculated with the following equation:

$$SOH = \frac{Q_{act}}{Q_{ref}} \times 100\% \tag{1}$$

B. Electrochemical impedance spectroscopy analysis

Electrochemical impedance spectroscopy (EIS) is one of the most important experimental tools in analyzing the lithium-ion batteries. As a non-destructive technique, EIS offers invaluable insights into the internal processes of a battery, facilitating the identification of various aging mechanisms. The measurement is based on exciting a battery cell with a sinusoidal signal of small amplitude. This involves using a current (galvanostatic) or voltage signal (potentiostatic). From the phase and amplitude shift between the input and output signal, the impedance for the excitation frequency is calculated. If this measurement is repeated over a wide frequency range, the impedance spectrum forms as a frequency-dependent curve, typically visualized using Nyquist plots [3].

After each capacity test, impedance spectra are measured at $25\,^{\circ}\mathrm{C}$ using potentiostatic EIS with an amplitude of $10\,\mathrm{mV}$ in a frequency range from $10\,\mathrm{mHz}$ to $10\,\mathrm{kHz}$. The measurement is conducted at $10\,\%$ SOC increments across the entire SOC range. The degradation of impedance parameters is quantified by extracting the ohmic (R_0) and polarization resistance (R_{pol}) from the spectra. This extraction is performed using the points-of-interest method, as proposed in [4] and demonstrated in Fig. 1. R_0 is determined by the intersection of the impedance spectrum with the real part axis. This value summarizes ohmic losses in the battery caused by surface contacts and the conductivity properties of used materials. R_{pol} is calculated by the difference between ohmic resistance and the real part of

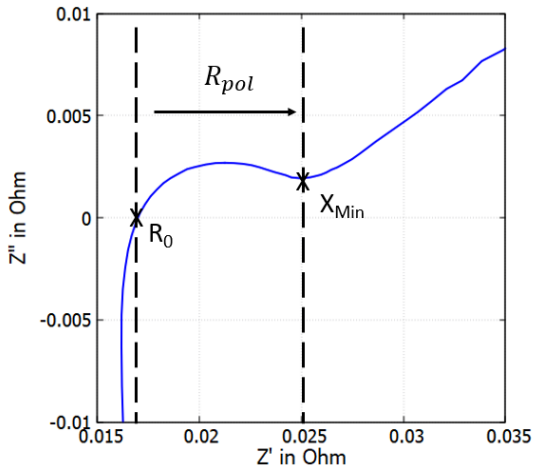

Fig. 1. Points of interest and calculation of polarization resistance in impedance spectrum (e.g. spectrum of LFP battery at 50 % SOC and $25\,^{\circ}\mathrm{C}$).

X_{Min} as shown in (2). X_{Min} marks the transition point from polarization to diffusion losses in the impedance spectrum. R_{pol} summarizes the charge transfer losses in interphase transitions and inside the active material of the electrodes.

$$R_{pol} = Re\{X_{Min}\} - R_0 \tag{2}$$

To minimize the numerical error arising from the limited number of measured frequency points in the detected points-of-interest, we initially refine the impedance spectra. The ripple of the impedance spectrum is preserved through a combination of linear and spline interpolation. First, the vectors of real part and frequency were refined through linear interpolation. Then, the corresponding values of the imaginary part were determined using cubic spline interpolation.

III. Design of Experiment

A. Lithium-Ion Battery Cell

We utilized a commercially available cylindrical cell with lithium-iron-phosphate (LFP / $LiFePO_4$) cathode chemistry and 21700 cell format. The cell has a nominal capacity of $3\,\mathrm{A\,h}$ (Q_{nom}), a nominal voltage of $3.2\,\mathrm{V}$ (U_{nom}) and can deliver a maximum constant current of $9\,\mathrm{A}$ (I_{max}^{const}). The detailed elemental composition, CT images, as well as the safety of the cells has been studied in [5]. The recommended charging protocol for the cells is CC-CV charging with a $1.5\,\mathrm{A}$ constant current rate, a maximum voltage of $3.65\,\mathrm{V}$. The maximum available constant charging current is $3\,\mathrm{A}$. The manufacturer guarantees a cycle life of at least 2000 cycles until the SOH reaches $70\,\%$ with the recommended charging protocol and a discharge rate of $1.5\,\mathrm{A}$ at room temperature.

B. Battery Experimental Setup

Cycling of the cells took place in a Basytec XCTS 24 Channel 25 Ampere cycler within a controlled environmental chamber. EIS, capacity and ohmic resistance analysis were performed using a Biologic BCS 815-128 test system with

Fig. 2. An inside view of the climate chamber: A single cell connected to the battery cycler.

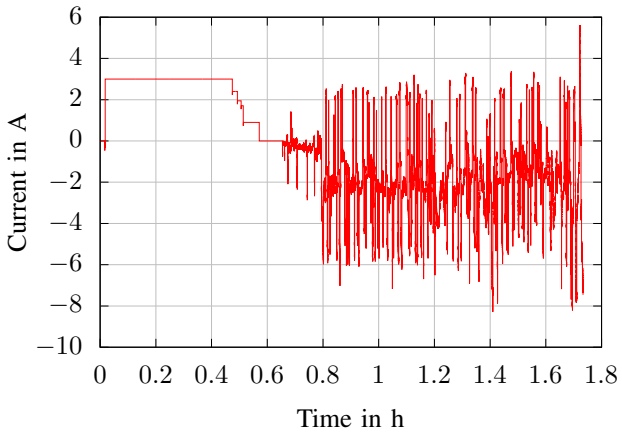

Fig. 3. Current profile for a segment of the high use realistic driving scenario.

corresponding cell holders. This system provides an 18-bit current and voltage resolution and enables high-precision EIS measurements over a frequency range of $10\,\mathrm{mHz}$ to $10\,\mathrm{kHz}$ on each channel [6]. Fig. 2 displays a cell connected to the cycler inside the environmental chamber.

C. Current Profiles for Testing

1) Standard Profiles: We conducted conventional cycling aging tests at $20\,^{\circ}\mathrm{C}$ to establish a reference for aging behavior. The cells are discharged with $1C$ and $2C$ rates within the range of $100\,\%$ to $0\,\%$ SOC and charged using the recommended CC-CV charging protocol. These protocols are referred to as Zyk1 and Zyk2, respectively. We utilized five cells for each profile. Capacity tests are implemented at each 100-cycle interval for Zyk1 and 50-cycle interval for Zyk2 to track the SOH of the cells.

2) Realistic Profiles: In our study, we employed an in-house developed tool, the "Realistic Driving Profile Generator" for the generation of realistic testing profiles [7]. The generator is designed in MATLAB/Simulink and utilizes online data sources. Initially, it generates speed and slope profiles for a specified route under consideration of speed limits, traffic signals, road intersections, and real-time traffic information. Subsequently, realistic current profiles are derived from the speed and slope profiles with an in-house developed EV drive train model, namely ETI Drive Train Model, according to the selected vehicle parameters. We simulated a compact electric vehicle, equipped with a 100 kW permanent-magnet synchronous motor and a 40 kWh battery operating at a nominal voltage of 400 V. A detailed description of the "realistic profile generator" can be found in [8].

Two realistic driving scenarios are utilized in this study. These chosen driving profiles represent two distinctive user behaviors. The "normal use" profile simulates the daily operation of an EV with a maximum discharge rate of $2C$ and battery charging conducted using the recommended CC-CV protocol. This profile consists of 96 road trips in Germany, incorporating a variety of route types and spanning a total distance of $2376\,\mathrm{km}$. Comprising $27\,\%$ of highways and $40\,\%$ of country roads, the proportional composition of the "normal use" data set mirrors the 2014 average usage statistics of passenger cars for Germany, as provided by the Federal Highway Research Institute of the Federal Ministry of Transport (BASt) [9]. On the other hand, the "high use" profile mimics the operational conditions of a commercial EV, where a significant portion of the simulated distance is covered on highways and the battery is charged using a fast-charging, Multi-Stage-Constant-Current (MSCC) protocol. In this case, we simulated the route between Karlsruhe and Leipzig, Germany. This route is $523\,\mathrm{km}$ long. Fig. 3 illustrates a segment of the current profile in the "high use" scenario, starting with the applied MSCC charging profile.

All the cells, for both normal use and high use, are cycled within an SOC range of $20\,\%$ - $100\,\%$ using the proposed profiles at $20\,^{\circ}\mathrm{C}$ ambient temperature.

IV. Experimental Results

The generated realistic profiles incorporate recuperation, employ different charging protocols and have a lower DOD of $80\,\%$ (between $100\,\%$ and $20\,\%$ SOC) compared to standard profiles. To enable a valid comparison, we used charge throughput instead of number of cycles for tracking the SOH. The cell manufacturer promises a minimum of 2000 cycles up to $70\,\%$ SOH, which can be converted to a charge throughput equivalent of $12\,\mathrm{kA\,h}$.

Fig. 4 shows the development of the SOH of the cells under the proposed test profiles. The End of Life (EOL) is defined at $80\,\%$ SOH and is marked with a red horizontal line. The slowest aging is observed with the Zyk2 protocol, where the EOL is achieved after approximately $11\,\mathrm{kA\,h}$ of charge throughput (CT). Cycling with Zyk1 results in an EOL after $8\,\mathrm{kA\,h}$. Both of the standard profiles comply with the cell manufacturer's commitments. On the other hand, the use of realistic profiles leads to significantly accelerated degradation. The cell cycled through the high use profile reach EOL after only $2.4\,\mathrm{kA\,h}$, indicating a lifespan approximately four times

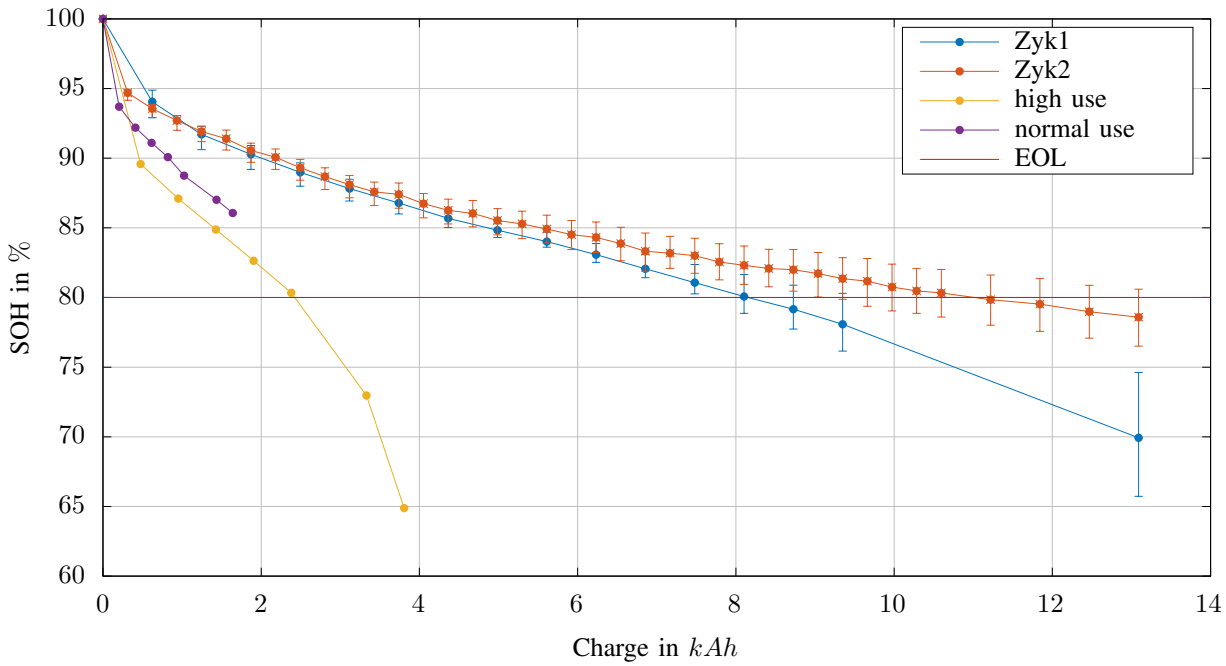

Fig. 4. Comparison of SOH loss due to cycling with standard and realistic profiles.

shorter than that under the Zyk1 and approximately five times shorter than under the Zyk2. These results are consistent with the mentioned literature. Baure and Dubarry also noted accelerated aging of NCA cells under the real driving loads. Similarly, S. Gantenbein reached the same conclusion in her investigation of the aging behavior of NCA and NMC cells in [10].

As anticipated, the high use profile accelerates aging slightly more than the normal use profile. This could be due to a combination of factors: fast-charging, a higher average current load, and higher cell temperature.

During the tests, the cell temperatures ranged from 21 °C - 24 °C for the normal use and 21 °C - 30 °C for Zyk1, 24 °C - 30 °C for the high use, and 21 °C - 36 °C for the Zyk2. Thus, the discrepancy between aging rates of realistic and standard profiles cannot be explained with temperature disparities. While higher temperatures typically accelerate aging, the cells tested under the normal use profile exhibited lower temperature range compared to those under standard profiles. Moreover, testing under high use and Zyk1 yielded similar temperature ranges. Although Zyk2 has the lowest aging rate, it exhibited the highest temperatures among all tests.

Hence, the durations of cyclic tests vary, we also investigated the effects of calendar aging. To understand its influence on the battery cell, storage tests were performed. Fig. 5 depicts the impact of calendar aging at 25 °C with both 30 % and 100 % SOC levels. After an initial sharp decrease in usable capacity, the rate of capacity loss diminishes over longer storage periods for both storage conditions. The cyclic test durations for Zyk1 and Zyk2 profiles were 525 and 490

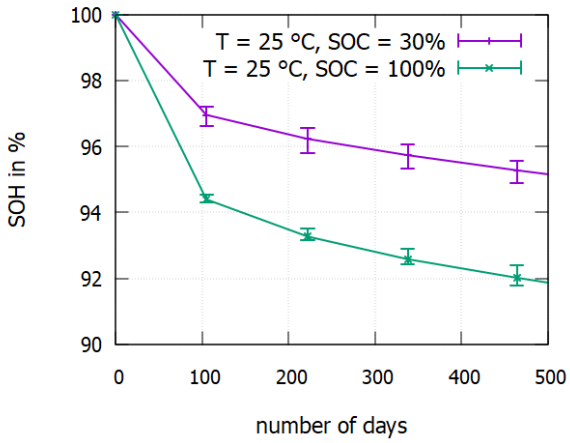

Fig. 5. SOH development by calendaric aging at T = 25 °C.

days, respectively. Calendar aging effects might be one of the reasons the cells perform better under Zyk2 than Zyk1 in Fig. 4. On the other hand, the normal use test spanned 210 days, while the high use test lasted 98 days. Test durations with realistic profiles are notably shorter than those with standard profiles, which in turn lessens the influence of calendar aging as a factor for accelerated degradation under realistic cycling. Ultimately, the recuperation phases, which are not included in the standard profiles, might be the reason of the accelerated aging observed under realistic profiles.

Fig. 6 visualizes the relative change of the ohmic and polarization resistances according to the SOH. The resistance

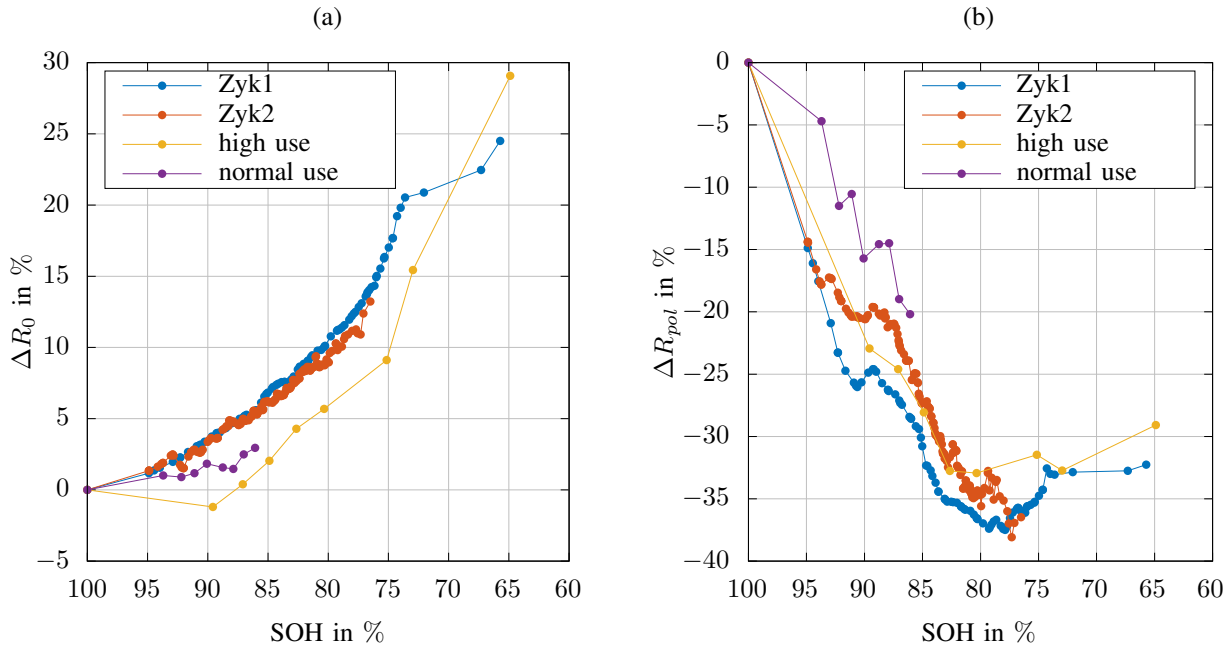

Fig. 6. Relative changes in ohmic (R_0) resistance (a) and polarization resistance (R_{pol}) (b) at 50 % SOC.

values were identified through EIS analysis at 50 % SOC, as introduced in II-B. Since the resistance values exhibit a minor dependency on the SOC within the mid-SOC range, any shift in the defined SOC levels due to degradation is neglected in the subsequent analysis. A clear increase in electrical losses is observable with the aging progression concerning the battery's ohmic resistance (R_0). Compared to Zyk1 and Zyk2, realistic profiles yield a less significant increase in R_0. With 6 % increase until the end of life (EOL), the rise obtained from high use cycling is approximately half the gain resulting from standard cycling. This might originate either in the amplification of lithium-consuming degradation processes or a decrease in electrolyte decomposition due to less time spent at low voltage levels within the cycle. A corresponding difference in voltage levels exists due to the different DOD of the used protocols. Cells cycled with standard profiles are discharged to an SOC of 0 %, whereas those subjected to realistic driving profiles are only discharged until they reach an SOC of 20 %. Lower voltage limits affect the electrochemical stability of the active material and amplify lithium plating, consequently causing an increase in ohmic resistance [11].

In our search for reasons for the amplified consumption of lithium, we are focusing on the evolution of the polarization resistance. The emergence of additional degradation processes, which consume active lithium, should manifest as a change in the course of the total charge transfer losses. As illustrated in Fig. 6, even though the cells under the high use profile experience the most rapid loss of active lithium, their polarization resistance demonstrates a trend similar to the cells cycled with Zyk1 or Zyk2. This observation suggests that while realistic driving profiles may significantly amplify lithium loss, the dominating degradation mechanisms causing the loss of lithium inventory (LLI) remain unchanged.

V. Conclusion

This study underscores the impact of realistic driving profiles on the aging behavior of $LiFePO_4$ batteries. The realistic load scenarios result in an accelerated aging rate compared to standard laboratory tests, demonstrating a more pronounced capacity loss. Interestingly, this discrepancy in aging rates could not be explained by temperature differences alone, pointing towards recuperation phases as a potential factor contributing to this accelerated aging. In search of the cause of accelerated aging, ohmic and polarization resistance have been analyzed using EIS-analysis. With declining SOH ohmic resistance shows an exponential growth, whilst polarization resistance decreases. Despite the more severe capacity loss, realistic cycling results in weaker gain of ohmic losses. This research underlines the necessity of using realistic driving profiles when assessing the life expectancy of EV batteries, with implications for improved battery management systems and enhanced longevity in real-world applications. Further studies are required to gain a more in-depth understanding of the effects of realistic load scenarios on battery aging and to develop effective mitigation strategies to extend the lifespan of batteries in EVs.

VI. Acknowledgment

This research was supported by the Helmholtz Association through the programs "Energy System Design" and "Materials and Technologies for the Energy Transition (MTET)". We

wish to express our gratitude for the funding provided. Additionally, this work is a contribution to the research undertaken at CELEST (Center of Electrochemical Energy Storage Ulm-Karlsruhe).

REFERENCES

[1] S. Panchal, J. Mcgrory, J. Kong, R. Fraser, M. Fowler, I. Dincer, and M. Agelin-Chaab, "Cycling degradation testing and analysis of a lifepo 4 battery at actual conditions," *International Journal of Energy Research*, vol. 41, no. 15, pp. 2565–2575, 2017.

[2] G. Baure and M. Dubarry, "Synthetic vs. real driving cycles: A comparison of electric vehicle battery degradation," *Batteries*, vol. 5, no. 2, p. 42, 2019.

[3] D. Andre, M. Meiler, K. Steiner, C. Wimmer, T. Soczka-Guth, and D. Sauer, "Characterization of high-power lithium-ion batteries by electrochemical impedance spectroscopy. i. experimental investigation," *Journal of Power Sources*, vol. 196, no. 12, pp. 5334–5341, 2011, Selected papers presented at the 12th Ulm ElectroChemical Talks (UECT):2015 Technologies on Batteries and Fuel Cells.

[4] H. Shabbir, W. Dunford, and T. Shoa, "State of health estimation of li-ion batteries using electrochemical impedance spectroscopy," in *2017 IEEE Transportation Electrification Conference and Expo (ITEC)*, IEEE, 2017, pp. 108–112.

[5] S. Ohneseit, P. Finster, C. Floras, N. Lubenau, N. Uhlmann, H. J. Seifert, and C. Ziebert, "Thermal and mechanical safety assessment of type 21700 lithium-ion batteries with nmc, nca and lfp cathodes; investigation of cell abuse by means of accelerating rate calorimetry (arc)," *Batteries*, vol. 9, no. 5, 2023.

[6] "BioLogic BCS-800 battery cycler series." (), [Online]. Available: https://www.biologic.net/products/bcs-800/.

[7] A. Kalk and J. Zhang, *Realistic driving profile generator*, Aug. 2023.

[8] A. Kalk, O. Birkholz, J. Zhang, C. Kupper, and M. Hiller, "Generating realistic data for developing artificial neural network based soc estimators for electric vehicles," in *2023 IEEE Transportation Electrification Conference (ITEC)*, 2023, pp. 1–7.

[9] M. Bauumer, H. Hautzinger, M. Pfeiffer, W. Stock, B. Lenz, T. G. Kuhnimhof, and K. Koehler, *Fahrleistungserhebung 2014 - Inlaenderfahrleistung* (Berichte der Bundesanstalt für Strassenwesen Fahrleistungserhebung 2014). Bremen: Fachverlag NW in der Carl Schuenemann Verlag GmbH, 2017.

[10] S. Gantenbein, "Impedanzbasierte modellierung von lithium-ionen zellen und deren degradationsverhalten," Dissertation, 2019.

[11] J. Vetter, P. Novak, M. R. Wagner, and C. Veit, "Ageing mechanisms in lithium-ion batteries," 2005.